

# Compound Dihuang Granule Protects against 6-OHDA Induced Toxicity in Parkinson's Disease Rats by Suppressing the Phosphorylation of MAPK/ERK1/2

**Li Wang**

Shanghai University of TCM: Shanghai University of Traditional Chinese Medicine

**Jian-ying Zhang**

Yunnan University of Traditional Chinese Medicine

**Long Chen**

Shanghai University of TCM: Shanghai University of Traditional Chinese Medicine

**Lei Zhang**

Shanghai University of TCM: Shanghai University of Traditional Chinese Medicine

**Zhu-qing He**

Shanghai University of TCM: Shanghai University of Traditional Chinese Medicine

**Peng-fei Huan**

Shanghai University of TCM: Shanghai University of Traditional Chinese Medicine

**Yu-fang Yang**

Shanghai University of TCM: Shanghai University of Traditional Chinese Medicine

**Jian-cheng He** (✉ [hejc8163@163.com](mailto:hejc8163@163.com))

Shanghai University of TCM: Shanghai University of Traditional Chinese Medicine

---

## Research

**Keywords:** Parkinson's disease, Compound Dihuang Granule, Oxidative stress, Apoptosis, MAPK/ERK1/2

**Posted Date:** September 2nd, 2021

**DOI:** <https://doi.org/10.21203/rs.3.rs-847269/v1>

**License:**  This work is licensed under a Creative Commons Attribution 4.0 International License.

[Read Full License](#)

---

# Abstract

## Background

Parkinson's disease (PD) is a multifactorial neurodegenerative disorder characterized by progressive loss of dopaminergic (DA) neurons in the substantia nigra pars compacta (SNpc) and the presence of Lewy bodies (LBs) consisting of misfolded  $\alpha$ -synuclein protein in the substantia nigra pars compacta (SNpc). Compound Dihuang Granule (CDG), a famous traditional Chinese medicine (TCM) has been clinically used in PD therapy with curative effects. However, the specific functions and the mechanism of action remained unclear. This study explored the therapeutic effects and potential mechanisms of CDG in the PD rats induced by 6-OHDA toxicity.

## Methods

The PD rat model was induced by unilaterally stereotactic injection of 6-OHDA into the SNpc of midbrain. The behavioral performances of rats were evaluated by rotation test, muscle strength assessment and balance beam walking test. The striatal contents of neurotransmitters were detected by HPLC. The numbers of dopaminergic (DA) neurons were determined with immunohistochemistry (IHC) staining and Western blotting assay. Indicators of oxidative stress were determined with colorimetric method. Apoptotic cells were detected by TUNEL assay. The expression levels of neurotrophic factors were examined with IHC staining and real-time quantitative PCR. The related protein expression levels were determined with Western blotting assay.

## Results

CDG significantly attenuated the 6-OHDA induced abnormal rotational behaviors and alleviated the loss of DA neurons in the nigrostriatal axis of PD rats with a 6-week treatment. Consistently, the striatal contents of DA and its metabolites including DOPAC and HVA of PD rats were all significantly increased with CDG treatment. The 6-OHDA induced oxidative stress indicated with decreased superoxide dismutase (SOD), glutathione (GSH), glutathione peroxidase (GSH-Px) and increased malondialdehyde (MDA) was also suppressed by CDG treatment. Moreover, CDG treatment increased the expression levels of neurotrophic factors including nerve growth factor (NGF), brain-derived neurotrophic factor (BDNF) and glial-derived neurotrophic factor (GDNF) in the nigrostriatal axis of PD rats. Consistently, the 6-OHDA induced cell apoptosis was inhibited by the 6-week CDG treatment. Further, the phosphorylation of MAPK/ERK1/2 and CREB proteins in the striatum of PD rats was suppressed by CDG treatment and CDG showed synergistic effects with the MAPK/ERK1/2 phosphorylation inhibitor SL327.

## Conclusion

CDG could ameliorate the 6-OHDA induced brain injuries and motor symptoms, and also inhibit the oxidative stress and cell apoptosis in the nigrostriatal axis, which was mainly mediated by enhancing the expression levels of the neurotrophic factors and suppressing the phosphorylation of MAPK/ERK1/2 pathway in the midbrain of rats.

# Introduction

PD is the second most common neurodegenerative disease with 2% of people aged over 60 years old suffering all over the world [1]. PD is clinically manifested with static tremor, bradykinesia, rigidity and abnormal posture [2], while pathologically characterized with progressive loss of DA neurons and deposition of  $\alpha$ -synuclein-containing lewy bodies (LBs) in the SNpc [3]. The etiology and pathogenesis of PD is complicated. So far, no treatment is available to effectively slow down or halt PD progression [3]. Levodopa is the only valid treatment reported to extend life expectancy of PD patients [4]. However, as long-term usage of the drug, the therapeutic effects become increasingly less beneficial, and more than 50% of patients eventually experience highly disabling fluctuations, dyskinesia and the agonist induced sleep attacks [5,6]. Therefore, it is imminent to find alternative therapy with less toxic side effects.

A variety of intracellular processes are involved in the pathogenesis of PD, including mitochondrial dysfunction, oxidative stress, cell apoptosis and neurotrophic factors deprivation [7,8]. Oxidative stress plays an undeniable role in the complex progressing neurodegenerative cascade, the inhibition of which attenuates DA neuron loss in PD models [7,8]. Neurotrophic factors are endogenous proteins promoting the survival of different neural cells [9], upregulation of which has been an effective approach for physical and medical treatments to protect against neurotoxicity induced neurodegeneration in PD [10,11]. Apoptosis is one of the main mechanisms responsible for neuronal deaths in PD. Apoptosis is mediated by a number of initiator and executioner caspases, and occurs via the intrinsic or extrinsic pathways [12]. The activation of MAPK/ERK1/2 has been commonly implicated in promoting neuroregeneration and cell apoptosis [13,14], in which the activation of CREB plays a synergetic role with the MAPK pathway [15,16].

Traditional Chinese medicine (TCM) is famous for the multidimensional clinical outcome in medical treatments. CDG has been clinically used in PD therapy for improving motor and non-motor symptoms and reducing the side effects of long-term Levodopa usage. CDG was proved to alleviate the excess levodopa induced dyskinesia in PD rat model [17]. In our previous study, CDG inhibited nigrostriatal pathway apoptosis in PD rats by suppressing the JNK/AP-1 Pathway [18]. And verbascoside, one of the main extracts of *Rehmannia glutinosa* root (the sovereign drug of CDG) was effective in treating PD and can increase the TH content of PD rats [19]. However, the protective effects and specific mechanisms of CDG in PD therapy remain to be further investigated.

In this study, the beneficial effects of CDG were documented in the 6-OHDA induced PD rats and the mechanisms of action were investigated. We evaluated the abnormal motor symptoms and the nigrostriatal loss of dopaminergic neurons of PD rats with or without CDG treatment. We found that CDG treatment significantly improved the 6-OHDA induced motor disorders and brain injuries of PD rats. Moreover, the 6-OHDA induced oxidative stress and cell apoptosis were alleviated by CDG treatment. CDG also increased the protein expression of the striatal neurotrophic factors. Further the inhibitor of MAPK/ERK1/2 was applied and we found that CDG significantly suppressed the MAPK/ERK1/2 phosphorylation in the striatum of PD rats. These findings elucidated that CDG treatment could improve

the Parkinsonian symptoms of the 6-OHDA induced PD rats, which was mainly mediated by the MAPK/ERK1/2 phosphorylation (Fig. 1).

## Materials And Methods

### Reagents

6-OHDA, Apomorphine, DA and DOPAC were purchased from Sigma Chemicals (St. Louis, MO, USA). Madopar was purchased from Shanghai Roche Pharmaceuticals Ltd (Shanghai, China). HVA was purchased from TCI (Shanghai) Chemical Industry Co., Ltd (Shanghai, China). Anti-Tyrosine Hydroxylase antibody-Neuronal Marker was purchased from Abcam (Cambridge, United Kingdom). SL327 was purchased from Shanghai Lanmu Chemical Co., Ltd (Shanghai, China). Primary antibodies ERK1/2, p-ERK1/2, CREB, p-CREB were purchased from Cell Signaling Technology Inc. (MA, USA). Primary antibodies NGF, BDNF, GDNF purchased from Abcam (Cambridge, United Kingdom). Oxidative stress injury was measured with biological kits purchased from Nanjing Jiancheng Biological Engineering Research Institute Co., Ltd (Nanjing, China). In situ cell death detection kit was purchased from Roche Molecular Systems, Inc. All other chemicals were commercially available and of reagent grade.

### Preparation of CDG

CDG was manufactured by Shanghai Traditional Chinese Medicine Pharmaceutical Technology Co., Ltd (Shanghai, China) (lot number, 20140102), which composed of Shu-Di-Huang, Bai-Shao, Gou-Teng, Zhen-Zhu-Mu, Dan-Shen, Shi-Chang-Pu and Quan-Xie in a dry weight ratio of 20:30:15:15:20:12:2 (table 1). The specific production steps of CDG referred to our previous research [18]. The quality control analysis of CDG was performed by LC-MS, which is stable and good repeatability (Fig. 2). The bioactive components of CDG was provided in supplementary material (Supplementary File S1). In the animal experiment, rats daily dosage of CDG was converted from human daily dosage with the equation  $DB \text{ (rat)} = DA \text{ (human)} * 7/388$ . Thus 6.3 times of the normal dosage for adult human was defined as the dosage of CDG for rats.

### Experimental Animals

Male Sprague-Dawley rats, weighing 160-200 g, were provided by the Animal Experimental Center of Shanghai University of TCM, China (license No. SYXK (Hu) 2020-0009). Rats were housed in wire cages at  $23 \pm 2^\circ\text{C}$  and 60-65% humidity, with illumination of 12-hour dark/light cycle (light 7:00-19:00, dark 19:00-7:00), with access to water and food ad libitum. All experimental procedures were conducted according to the National Institute of Health Guide for the Care and Use of Laboratory Animals, and approved by the Animal Care Committee of Shanghai University of TCM. And the method to establish the 6-OHDA induced PD model was referred to our previous research [18].

### Drug Treatments

Rats in the CDG group were intragastrically given 7g/kg/d CDG (1 mL/100 g), and 10% DMSO was injected intraperitoneally. Rats in Madopar group were gavaged with 150 mg/kg Madopar and 10% DMSO was injected intraperitoneally. Rats in the SL327 group were intraperitoneally given 25 mg/kg SL327 solution (dissolved in 10% DMSO) and gavaged with 1 mL/100 g of saline. Rats in the CDG + SL327 group were intraperitoneally given 25 mg/kg SL327 immediately after gavage with 7 g/kg/d CDG. Rats in the sham group and Model group were gavaged with 1 mL/100 g of saline and intraperitoneally given 10% DMSO solution. The intraperitoneal injection volume was 0.1 mL/100 g, twice weekly for 6 weeks.

## **Behavioral tests**

### **Rotation test**

Two weeks after the operation, the rats' contralateral rotations induced by Apomorphine (APO) were measured and recorded with a video camera at 2 weeks, 4 weeks and 6 weeks. The duration of each recording time was 30 min. Rats with a rotating frequency of over 7 turns per minute were included in the PD model[20].

### **Muscle strength assessment**

Take a wire rope (length 100cm, diameter 0.15cm), fix its two ends, 70cm away from the ground, and put down a sponge pad (5cm thick) to prevent rats from falling. During the operation, the rat's two front paws were placed on the wire rope, and then let go, observe the rat's behavior, and record its suspension time. Use the following points to evaluate the muscle strength of the experimental rats: 3 points, hanging on the rope for more than 5s, and the hind limbs can be placed on the rope; 2 points, hanging on the rope for more than 5s; 1 point, hanging on the rope 3~4s; 0 points, hanging on the rope 0~2s.

### **Balance beam walking test**

The rats walked the entire length of a standard balance beam (80 cm in length, 2.5 cm in width, 100 cm off the floor) steadily without falling off [21,22]. Briefly, a subjective observation was conducted for 60 seconds. Score 0 indicates stable balance; score 4 indicates fall off. The test was performed in triplicate on weeks 0, 2, 4 and 6. The average score of balance of each rat was calculated.

### **High performance liquid chromatography (HPLC)**

After the behavioral test, the striatum was homogenized in 0.4 mol·L<sup>-1</sup> perchloric acid solution (1 mg: 40 μ L). After centrifugation at 12000 r/min for 15 min at 4 °C, the supernatant was collected and placed on ice until further HPLC analysis. The chromatographic conditions were as follows: the Welch XB-C18 column (4.6×250 mm, 5 μ m); mobile phase: 6% methanol, 0.035 mol·L<sup>-1</sup> anhydrous citric acid, 0.09 mol·L<sup>-1</sup> sodium acetate anhydrous, 0.23 mmol·L<sup>-1</sup> sodium octyl sulfonate, 0.13 mmol·L<sup>-1</sup> EDTA. and pH=4.1; flow rate: 1 mL/min; and injection volume: 50 μ L.

## Liquid chromatography - mass spectrometry (LC-MS)

Analysis platform: LC-MS (Thermo, Ultimate 3000LC, Orbitrap Elite); Column: ACQUITY UPLC HSS T3 (100x 2.1 mm, 1.7  $\mu$  m); Chromatographic separation conditions: Column temperature: 40 °C; Flow rate: 0.3 mL/min; Mobile phase A: water SP 0.1% formic acid; Mobile phase B: acetonitrile SP 0.1% formic acid; Injection volume: 4  $\mu$  L; Automatic injector temperature: 4 °C. The gradient was 5~95% Mobile phase B over 11 min, 95% Mobile phase B over 11~15 min, 95~5% Mobile phase B over 15-15.5 min, 5% Mobile phase B over 15.5~19.5 min. ESI+: Heater Temp 300 °C; Sheath Gas Flow rate, 45arb; Aux Gas Flow Rate, 15 arb; Sweep Gas Flow Rate, 1arb; spray voltage, 3.0 KV; Capillary Temp, 350 °C; S-Lens RF Level, 30%. ESI-: Heater Temp 300 °C, Sheath Gas Flow rate, 45arb; Aux Gas Flow Rate, 15arb; Sweep Gas Flow Rate, 1arb; spray voltage, 3.2 KV; Capillary Temp, 350 °C; S-Lens RF Level, 60%.

## Western blotting analysis

The striatum tissues were lysed in T-PERTM Tissue Protein Extraction Reagent (Thermo Scientific, USA) containing complete protease inhibitor. Protein concentrations were measured using a BCA kit (Beyotime, Shanghai, China). 40  $\mu$  g of protein from each group was separated by 10% SDS-PAGE gels and electrophoresis and subsequently transferred onto a PVDF membrane (0.45  $\mu$  m, EMD Millipore, MA, USA). BSA (3%; Sigma-Aldrich, MO, USA) was used to block the membranes for 2 h at room temperature (RT). The membranes were then incubated with primary antibody TH, Bax, Bcl-2, ERK1/2, p-ERK1/2, CREB, p-CREB (CST, MA, USA) overnight at 4 °C. After the membranes were washed three times with tris-buffered saline containing 0.1% Tween-20 (TBST), they were incubated with the horseradish peroxidase-conjugated secondary antibody mouse  $\beta$ -Actin, GAPDH Antibody Mouse Monoclonal (Proteintech, Rosemont, USA) for 1 h at RT. After the final wash, signals were detected using Li-cor ODDSEY infrared laser imaging system (CLx-1259, LI-COR Biosciences, USA); Image J software was used to analyze the strip optical density.

## Detection of mRNA expression by real-time fluorescence quantitative PCR

The total RNA of the rats in each group were extracted with RNAiso Plus and were transformed into cDNA by reverse transcription kit (Takara, Beijing, China) according to the manufacturer's protocol. RT-PCR was performed on ABI StepOnePlus real-time fluorescent quantitative PCR system (ABI StepOnePlus USA). Taking  $\beta$ -actin as the endogenous reference, the relative amount of mRNA is determined based on  $2^{-\Delta\Delta CT}$  calculation. The primer sequences of TH, GDNF, BDNF, NGF were listed in Table 2.

## Immunohistochemistry (IHC)

The 20- $\mu$ m-thick slices of rat brain tissue from each group were selected as similar as possible. And frozen slices were subjected to citrate buffer (0.1 M, pH 6.0) at 95 °C for 10 min for antigen retrieval. After the tissue was washed three times with phosphate-buffered saline containing 0.2% Tween-20 (PBST) for 10 min, the sections were treated with 0.5% Triton X-100 for 10 min and blocked with 5% bovine serum albumin (BSA) for 1 h at RT. After blocking, the sections were incubated with anti- mouse TH (Cambridge,

MA, USA), which was prepared with PBST (0.5% Triton X-100) /1% sheep serum, incubated at 37 °C for 2 h, 4 °C overnight. Then, samples were incubated with the horseradish peroxidase-conjugated secondary antibody (Cambridge, MA, USA) for 1 h, and samples were detected with 3,3'-diaminobenzidine (DAB) for 2-3 min. Finally, the sections were cover-slipped with neutral balsam and observed with an Olympus BA51 photomicroscope (Tokyo, Japan). Image Pro Plus 6.0 software (Media Cybernetics, MD, USA) was used for cell counting. For the detection of neurotrophic factors, the 3.5- $\mu$ m-thick paraffin sections were mounted on glass slides and baked for 1h at 62 °C, after which they were deparaffinized and the endogenous peroxidase activity quenched. The primary antibody NGF (Abcam, UK), BDNF (Abcam, UK), GDNF (Abcam, UK) was incubated on the slides for 12 h at 4 °C. After rinsing three times with phosphate-buffered saline solution containing Tween, the horseradish peroxidase-conjugated secondary antibody (Huaan, Hangzhou, China) was incubated for 20 min at RT and then visualized after incubation with 3, 3'-diaminobenzidine for 10 min at RT. Then the sections were counterstained with hematoxylin to mark the nucleus. Finally, the binding sites were sealed with neutral resin. Images were obtained at the objective len with 20 $\times$  magnification. The numbers of positive cells were counted Image J software.

### **Immunofluorescence staining**

Brain frozen slices with 20 $\mu$ m thick from each group were washed with PBS five times for 3 min each. Then, 0.5% (wt/vol) Triton X-100 and blocking serum were added successively and incubated for 10 min and 1.5 h, respectively. The tissue was incubated in primary antibody, anti- mouse TH (Cambridge, MA, USA), at 4 °C overnight. After being washed four times with PBS, the sections were incubated with the secondary antibody (Alexa Fluor 488; A-11007, Alexa Fluor 555; Invitrogen, CA, USA) for 1h at RT and protected from light. Images were obtained with confocal microscopy. The number of positive cells was calculated with Image J software.

### **Measurement of oxidative stress**

Rats from each group were anesthetized with pentobarbital sodium (50 mg/kg), decapitated and their brains removed, then the right substantia nigra was dissected out and weighed. (1) removal of the brain 0.5 g in the cold saline to remove blood, rinse, dry filter paper, then put in the specifications for 5mL small beaker; (2) adding 0.65 mL cold 0.9% saline in the beaker, and with ophthalmic scissors cutting brain block. as soon as possible; The brain tissue suspension was then poured into the homogenate tube, and the cold 0.86% saline 0.3 mL was added to the homogenate of 3~5 min, and the 10% brain tissue homogenate was prepared, and centrifuged at 12,000 $\times$ g for 10 minutes at 4 °C; The above steps were carried out on the ice. Take proper amount of supernatant of SOD, MDA, GSH, GSH-Px detection, the specific methods of operation in strict accordance with the completion of Nanjing Institute of biological engineering kit (Nanjing, China) detection steps.

### **TUNEL assay**

Select appropriate brain slices from each group of rats from the in situ hybridization protection solution. TUNEL staining was performed as described previously according to the manufacturers' protocols with

minor modifications. Briefly, TUNEL assay was performed in 20- $\mu$ m-thick frozen sections using in situ cell death detection kit (Roche, Switzerland Basel, Germany). All images were acquired using a confocal microscope (Leica TCS SP2, Solms, Germany). The nuclei were stained with DAPI (blue), and the apoptotic cells appeared green. Image Pro Plus 6.0 software (Media Cybernetics, MD, USA) was used for cell counting.

## Statistical analysis

The experimental data statistics are expressed as mean  $\pm$  standard error (Means  $\pm$  SEM). Two groups of data were compared using t test, and multiple groups of data were analyzed by One-way ANOVA or Two-way ANOVA followed with Turkey's multiple comparison test post hoc. When  $P < 0.05$ , there was statistical difference.

## Results

### CDG ameliorated behavioral symptoms of 6-OHDA induced PD rats

With induction of APO, no rotational behavior was observed throughout the test in sham-operated rats, while the number of the rotations of PD rats significantly increased after surgery and gradually decreased week by week ( $P < 0.001$ ). The number of rotations of the Madopar group decreased significantly compared with 6-OHDA-lesioned group ( $P < 0.01$ ) at 6 weeks. With 4 weeks, and 6 weeks of treatment, the number of rotations of the CDG group and Madopar group significantly decreased compared with the model group ( $P < 0.001$ , Fig.3). There was no significant difference in the number of rotations between the Madopar group and the CDG group ( $P > 0.05$ ). These results suggested that CDG reduced motor dysfunction in PD rats.

### CDG attenuated nigrostriatal dopamine loss of PD rats

Loss of striatal DA and its metabolites is closely related to the dyskinesia of PD. In this study, the striatal contents of neurotransmitter DA and the intermediate metabolites including DOPAC and HVA were determined with HPLC. Compared with the Sham, 6-OHDA toxicity induced a significant reduction of DA, DOPAC, and HVA levels in the striatum of Model rats. Compared with the Model group, the striatal contents of DA, DOPAC and HVA all increased significantly in both the Madopar and CDG group ( $P < 0.01$ , Fig.4 A-C), however there was no difference between the two groups ( $P > 0.05$ ). These results showed that CDG treatment increased the contents of neurotransmitters including DA, DOPAC and HVA in the striatum of 6-OHDA induced PD rat.

To examine the DA neuronal injuries in the SNpc of PD, the protein expression of TH in striatum was determined. Compared with the sham-operated groups, the expression of TH protein in the striatum of PD rats was significantly decreased ( $P < 0.01$ ). With 6-week treatment of Madopar or CDG, the protein expression levels of TH were significantly increased in the striatum of PD rats ( $P < 0.05$ ,  $P < 0.01$ , Fig. 4 D-

E). However, there was no significance between the Madopar and CDG group ( $P>0.05$ ). These results suggested that CDG increased TH protein expression in the nigrostriatal pathway of PD rats.

### **CDG attenuated 6-OHDA induced loss of nigrostriatal DA neurons in the PD rats**

Immunohistochemistry staining was used to evaluate the injuries of nigrostriatal DA neurons (Fig. 5 A-C). The number of DA neurons in the SNpc of Model rats significantly decreased compared with the Sham group. Compared with the model group, the number of DA neurons increased significantly in the SNpc of rats with Madopar or CDG treatment ( $P<0.05$ ). In addition, the density of TH neuronal terminals in the striatum of rats was calculated. With 6-OHDA toxicity, the TH average optical density (AOI) of the striatum significantly decreased in the Model rats, while both CDG and Madopar treatment improved the density of TH neuronal terminal in the striatum of PD rats. However, there was no significance between the two groups ( $P>0.05$ ). These results demonstrated that CDG treatment could attenuate the 6-OHDA induced DA neuronal injuries.

### **CDG alleviated 6-OHDA induced oxidative stress in the Striatum of PD rats**

Compared with the Sham group, the SOD content, GSH and GSH-Px activity in the striatum of the Model group decreased significantly, while the MDA level significantly increased; Compared with the Model group, the MDA level of rats in the CDG and Madopar group significantly decreased, while the SOD content, GSH and GSH-Px activity significantly increased (Fig. 6 A-D). However, there was no significance between CDG and Madopar group ( $P>0.05$ ). These results showed that CDG alleviated oxidative stress in PD rats.

### **CDG increased the expression of neurotrophic factors in the SNpc of PD rats**

The protein expression levels of neurotrophic factors including NGF, BDNF and GDNF were determined with immunohistochemical staining in the SNpc of PD rats, and the cell counting was conducted. Compared to the Sham group, the number of NGF positive cells was significantly decreased in the SNpc of Model group (Fig.7 A), while both Madopar and CDG treatment efficiently rescued this decline as indicated by the statistical analyses (Fig.7 B). Moreover, the increase of NGF positive cells was more significant in the CDG group than the Madopar group, when compared to the Model ( $P<0.01$  and  $P<0.001$ ), however the changes between the two groups are identical. Changes of BDNF and GDNF positive cells in the SNpc of four groups were consistent with the NGF expression (Fig.7A, C&D). The results suggest that CDG treatment significantly increased the protein expression levels of the neurotrophic factors including NGF, BDNF and GDNF in the nigrostriatal pathway of 6-OHDA induced PD rats.

### **CDG reduced 6-OHDA induced cell apoptosis in the nigrostriatal pathway of PD rats**

In view of the decreased oxidative stress injuries and increased expression of neurotrophic factors in the CDG treated rats' brains, we wonder that if CDG could reduce 6-OHDA induced cell deaths. The apoptotic cells in the SNpc were examined with TUNEL assay (Fig. 8 A-B). Co-staining with TH (red) protein, the

apoptotic neurons in the SNpc of rats were marked by TUNEL (green) assay. Compared with Sham group, the number of apoptotic neurons significantly decreased in the SNpc of Model rats ( $P<0.001$ ), however this decline was significantly attenuated by Madopar treatment ( $P<0.05$ , Model vs. Madopar). Moreover, the CDG treatment showed identical effects with Madopar, which is more significant for reducing the apoptotic neurons in the SNpc ( $P<0.01$ , Model vs. CDG).

Meanwhile, the protein expression levels of Bcl-2 and Bax in the striatum of rats were determined with Western blotting assay (Fig. 8 C-D). Compared with Sham group, Bax protein significantly increased while Bcl2 protein decreased in the striatum of Model group. Consistently, the ratio of Bcl2/Bax protein expression significantly decreased in the striatum of Model group, ( $P<0.001$ ). Corresponding to the number of apoptotic neurons in the SNpc, changes of Bax and Bcl2 protein induced by 6-OHDA toxicity were both attenuated with Madopar and CDG treatment ( $P<0.05$  and  $P<0.01$  respectively). Together, the results showed that CDG treatment could suppress the apoptosis of dopaminergic neurons in the nigrostriatal pathway of 6-OHDA induced PD rats.

### **The parallel effects between CDG and SL327 in 6-OHDA induced PD rats**

Neuroregeneration and Cell apoptosis were widely reported to be regulated by the MAPK/ERK1/2 phosphorylation [23-25], thus we further investigated that if CDG treatment delivered its protective effects by regulating the MAPK/ERK1/2 pathway with introducing the MAPK/ERK inhibitor SL327.

The behavioral performances of rats were examined including the Apomorphine induced rotation test, muscle strength assessment and balance beam walking test. SL327 or CDG each alone significantly alleviated the abnormal rotation behaviors of Model rats since the treatment of 2 weeks, 4 weeks and 6 weeks ( $P<0.05$ ), while their combined utilization showed more prominent effects (SL327+CDG vs. SL327 or CDG,  $P<0.05$ ; Fig .9 A-C). In the balance beam walking test, compared with Sham group, all other groups of rats spent much more time crossing the beam, suggesting the motor deficits induced by unilateral injection of 6-OHDA into the SNpc. However, compared with the Model group, SL327, CDG and their combined usage all showed improving effects with a 6-week treatment ( $P<0.05$  each), although the improvements among three groups were identical (Fig .7 B). In the muscle strength assessment, the score of Model rats significantly decreased compared to the Sham rats since the 6-OHDA injection. CDG significantly improved the performances of model rats with 2 weeks, 4 weeks and 6 weeks of treatment, while SL237 showed no effect neither by single usage nor combined with CDG ( $P<0.001$ ) (Fig .9 C).

To further evaluate the effects of CDG on suppressing the MAPK/ERK phosphorylation, the striatal expression levels of TH of rats were determined with Western blotting and real-time quantitative PCR (Fig.9 D-F). As expected, compared to the Sham group, the striatal TH protein significantly decreased in the Model rats (Sham vs. Model,  $P<0.001$ ), however SL327, CDG and their combined usage all attenuated the loss of TH proteins (each vs. Model,  $P<0.05$ ) and there was no difference among the three groups (Fig .9 E-F). Consistently, the striatal mRNA levels showed the same changes with the results of TH protein expression. All-together, CDG and SL327 both significantly improved the motor symptoms and striatal DA loss of 6-OHDA induced PD rats, and their combined usage showed even promoted effects,

suggesting that CDG had similar protective effects in common with the MAPK/ERK1/2 phosphorylation inhibitor.

### **CDG inhibited the phosphorylation of MAPK/ERK1/2 induced by 6-OHDA toxicity**

Protein expression levels of the upstream regulatory MAPK/ERK1/2 and CREB proteins were determined (Fig. 10A-C). The striatal protein expression levels of ERK and CREB were similar among all groups. Compared with the Sham, the phosphorylation of ERK and CREB both significantly increased in the striatum of Model rats, which was significantly inhibited by SL327 treatment. The CDG treatment showed similar effects on suppressing the ERK and CREB phosphorylation. Moreover, the combined utilization of CDG and SL327 enhanced the inhibition of CREB phosphorylation than the SL327 alone, indicating the synergistic effects of CDG with SL327. Therefore, the results showed that CDG could suppress the phosphorylation of MAPK/ERK1/2 and CREB and enhance the inhibitory effects of MAPK/ERK1/2 inhibitor SL327.

The mRNA expression levels of these neurotrophic factors in the striatum of rats were further examined. Corresponding to the protein expression levels of the neurotrophic factors, the striatal mRNA level of NGF, BDNF, and GDNF in the Model group all significantly decreased compared with the Sham group, which was significantly rescued with SL327 or CDG treatment. However, the combined utilization of both showed no better effect than each alone (Fig.10 D-F). Taken together, MAPK/ERK1/2 signaling pathway is involved in the protective effects of CDG treatment against the 6-OHDA toxicity.

## **Discussion**

The incidence of PD increases greatly in the worldwide, and a large number of studies have shown that TCM treatment could not only improve the clinical efficacy but also reduce the side effects of chemically synthesized drugs in PD therapy [26]. CDG has been clinically applied in the PD treatments and significantly improve the UPDRS score of PD patients compared to the patients with single Madopar treatment [27]. In our previous study, CDG was proved to alleviate the excess levodopa induced dyskinesia in PD rat model [17]. Moreover, CDG inhibited the nigrostriatal pathway apoptosis of PD rats by suppressing the JNK/AP-1 Pathway [18]. In this paper, the protective effects of CDG in PD were systematically studied in a 6-OHDA toxicity induced PD rat model. We obtained experimental evidences that CDG attenuated the nigrostriatal DA loss, improved oxidative stress, inhibited cell apoptosis and increased the expression of neurotrophic factors in the 6-OHDA induced PD rats, demonstrating the protective role of CDG in PD therapy, and which was mainly mediated by suppressing the phosphorylation of MAPK/ERK1/2.

Herein, the protective effects of CDG for PD were proved in the rat model induced by unilateral injection of 6-OHDA into the medial forebrain bundle and SNpc. 6-OHDA selectively damages dopaminergic neurons with prolonged injuries, the toxicity of which is frequently used to construct in vivo and in vitro Parkinson's disease models. The protective effects of *L. stoechas* methanol extract were investigated on 6-OHDA-induced cytotoxicity and oxidative damage in PC12 cells [28]. In this study, the PD rat model with

prolonged DA neuronal damages allowed the delivery of 6-week treatment even longer, in which the rotational behaviors and loss of DA neurons were alleviated, and the DA neurotransmitter with its metabolites including DOPAC and HVA were significantly increased by CDG treatment. Therefore the therapeutic effects of CDG were well demonstrated for alleviating parkinsonian appearances.

Madopar was applied in this study as a positive control, the 6-week treatment of which delivered similar protective effects in 6-OHDA induced PD rats. Madopar consisting of two active ingredients called levodopa and benserazide, has been clinically applied in PD therapy for improving the clinical symptoms [29]. In this study, the PD rat model with prolonged DA neuronal damages allowed the delivery of a 6-week treatment even longer, in which the rotational behaviors and loss of DA neurons were alleviated, and the DA neurotransmitter with its metabolites including DOPAC and HVA were significantly increased by Madopar and CDG treatment. The improvements of PD rats were even more significant with CDG treatment than that with Madopar treatment in the examination of behavioral performances and cell apoptosis in the PD rats. Therefore CDG showed comparable therapeutic effects to Madopar in the 6-OHDA induced PD rats.

Overwhelming evidences suggest that oxidative stress plays a vital role in the degeneration of dopaminergic neurons, the suppression of which directly protects the DA neurons in midbrain [7]. In this study, 6-OHDA induced the increase of MDA and the decrease of antioxidants including SOD, GSH and GSH-Px in the striatum, however the induced oxidative stress was all reversed by the CDG treatment, suggesting the protective effects of CDG against the oxidative stress injuries. Neurotrophic factor (NTFs) could reduce neuronal apoptosis and promote the neurite regeneration [30]. BDNF promotes the survival, differentiation and growth of DA neurons [31]. In this study, CDG significantly increased the numbers of NGF, BDNF and GDNF positive neurons in the SNpc of PD rats, and also increased the mRNA expression levels of the NTFs in the striatum of PD rats, thereby revealing one of the neuroprotective mechanisms of CDG for increasing the expression of the neurotrophic factors in the brain. The Bcl-2 protein family including the pro-apoptotic proteins (such as Bax) and anti-apoptotic proteins (such as Bcl-2) play a vital role in the process of apoptosis [32]. With exposure to the oxidative stress, pro-apoptotic proteins will translocate to the outer membrane of mitochondria, triggering the release of apoptosis-inducing factors, thus inducing apoptosis [33]. The TUNEL-positive neurons in the SNpc of 6-OHDA induced PD rats were significantly decreased with CDG treatment, as well as the increased expression of Bcl-2/Bax protein, suggesting the protective role of CDG against cell apoptosis. However, the specific mechanisms were still undefined.

The molecular mechanisms involved in the protective effects of CDG were further discovered. By introducing the inhibitor of MAPK/ERK1/2 pathway, the role of CDG in regulating the ERK phosphorylation was studied. CDG significantly inhibited the phosphorylation of ERK protein and the upstream molecule CREB protein in the striatum of the PD rats, which was similar with the effects of ERK inhibitor SL327, demonstrating the suppression of CDG for MAPK/ERK1/2 in the 6-OHDA induced injuries. Moreover, the effects of CDG were compared with SL327 by examining the behavioral performances and brain injuries of PD rats. SL327 also showed protective effects in attenuating the

motor deficits and striatal TH loss of PD rats. However, the CDG treatment alone or the combination use of CDG and SL327 either showed better effects than SL327 alone in improving the rotational behaviors of rats. Therefore, CDG played a synergetic role with the SL327 in alleviating the motor symptoms of 6-OHDA induced PD rats. Whereas CDG alone showed better effects than SL327, indicating that CDG orchestrated not only the MAPK/ERK1/2 pathway to deliver the protective effects on 6-OHDA induced brain injuries, which was consistent with the multifaceted actions of TCM. In conclusion, CDG treatment can alleviate DA neuron loss and motor deficits of PD by suppressing the phosphorylation of MAPK/ERK1/2 signaling pathway.

## Conclusions

In summary, this study reveals that CDG, a compound traditional Chinese medicine, protected against the Parkinsonian pathologies in the 6-OHDA induced PD rats, with improving the neurobehavioral performance of PD rats and attenuating the nigrostriatal loss of DA neurons. Moreover, the oxidative stress and cell apoptosis induced by 6-OHDA toxicity were also ameliorated by CDG treatment. CDG increased the expression of neurotrophic factors while inhibited the phosphorylation of MAPK/ERK1/2 and CREB proteins in the nigrostriatal pathway of PD rats, implicating the potential mechanisms of action. Collectively, these results provide evidences for the protective role of CDG treatment in PD therapy, which extends our understanding on the treatments of neurodegenerative diseases with traditional Chinese medicine.

## Abbreviations

PD: Parkinson's disease; CDG: Compound Dihuang Granule; DA: Dopamine; SNpc: Substantia nigra pars compacta; DOPAC: 3,4-dihydroxyphenylacetic acid; HVA: Homovanillic acid; IHC: Immunohistochemistry; DRT: Dopamine replacement therapy; TCM: Traditional Chinese medicine; HPLC: High performance liquid Chromatography; EC: Electrochemical detection; RT: Room temperature; BSA: Bovine serum albumin; SOD: Supernatant of superoxide dismutase; MDA: Malondialdehyde; GSH: Glutathione; GSH-Px: Glutathione peroxidase; APO: Apomorphine; DAT: Dopamine transporter; 6-OHDA: 6-hydroxydopamine; TH: Tyrosine hydroxylase; Bax: Bcl-2 associated X; Bcl-2: B-cell lymphoma-2; DAB: 3,3'-Diaminobenzidine; DAPI: 4,6-Diamidino-2-Phenylindole; TUNEL: Transferase-mediated deoxyuridine triphosphate-biotin nick end labeling; MPTP: 1-Methyl-4-phenyl-1,2,3,6-tetrahydropyridine; SNpc: substantia nigra pars compacta; LC-MS: Liquid chromatography - mass spectrometry;

## Declarations

### Acknowledgments

We thank Dr. Yanwu Xu (Shanghai University of TCM) for proofreading and editing.

### Author's contributions

Each author has contributed significantly to this study. JH, YY, JZ and LW conceived and designed the study. LW, JZ and LC performed the animal and molecular biology experiments. ZH, PH and LZ performed the statistical analyses. LW drafted the manuscript. LW and YY revised the manuscript. All authors read and approved the final manuscript.

## **Funding**

This research was supported by the National Natural Science Foundation of China (No. 81573899), the Shanghai Sailing Program (No.19YF1448500) and the General project of China Postdoctoral Science Foundation (No.2019M651562).

## **Declaration of competing interest**

All authors of this manuscript state that they do not have any conflict of interests, and there is nothing to disclose.

## **Availability of data and materials**

Please contact corresponding authors for data requests.

## **Ethics approval and consent to participate**

All procedures in this study were approved and supervised by the animal research ethical committee of Shanghai University of TCM, and strictly obeyed the rules of animal experiment ethic to reduced number as well as suffering of animals.

## **Consent for publication**

Not applicable.

## **Competing interests**

The authors declare that they have no competing interests.

## **Author details**

<sup>1</sup> Department of Diagnostics of Traditional Chinese Medicine, School of Basic Medicine, Shanghai University of Traditional Chinese Medicine, Shanghai, 201203, China. <sup>2</sup> Experiment Center, Shanghai Municipal Hospital of Traditional Chinese Medicine, Shanghai University of Traditional Chinese Medicine, Shanghai, 200071, China. <sup>3</sup> School of Basic Medicine, Yunnan University of Traditional Chinese Medicine, Kunming,650500, China. <sup>4</sup> Experiment Center for Science and Technology, Shanghai University of Traditional Chinese Medicine, Shanghai, 201203, China. <sup>5</sup> Shanghai Key Laboratory of Health Identification and Assessment, School of Basic Medicine, Shanghai University of Traditional Chinese Medicine, Shanghai, 201203, China.

# References

- 1.Jankovic, J., & Tan, E. K. Parkinson's disease: etiopathogenesis and treatment. *J Neurol Neurosurg Psychiatry*.2020;91(8) :795-808.
- 2.Armstrong MJ, Okun MS. Diagnosis and treatment of Parkinson disease. *JAMA*.2020;323:548-560.
- 3.Chen Z, Li G, Liu J.Autonomic dysfunction in Parkinson's disease: Implications for pathophysiology, diagnosis, and treatment. *Neurobiol Dis* .2020;134:104700.
- 4.Poewe W, Espay AJ. Long duration response in Parkinson's disease: levodopa revisited. *Brain*. 2020;143(8):2332-2335.
- 5.Reich SG, Savitt JM. Parkinson's Disease. *Med Clin North Am*. 2019;103(2) :337-350.
- 6.Zuzuárregui JRP, During EH. Sleep Issues in Parkinson's Disease and Their Management. *Neurotherapeutics* .2020;17(4) :1480-1494.
- 7.Trist, B.G., Hare, D.J., and Double, K.L. Oxidative stress in the aging substantia nigra and the etiology of Parkinson's disease. *Aging Cell*.2019;18: e13031.
- 8.Lin, C.H., Wei, P.C., Chen, C.M., Huang, Y.T., Lin, J.L., Lo, Y.S., Lin, J.L., Lin, C.Y., Wu, Y.R., Chang, K.H., and Lee-Chen, G.J. Lactulose and Melibiose Attenuate MPTP-Induced Parkinson's Disease in Mice by Inhibition of Oxidative Stress, Reduction of Neuroinflammation and Up-Regulation of Autophagy. *Front Aging Neurosci*.2020;12: 226.
- 9.Chmielarz P, Saarma M. Neurotrophic factors for disease-modifying treatments of Parkinson's disease: gaps between basic science and clinical studies. *Pharmacol Rep*.2020; 72(5) :1195-1217.
- 10.Shadfar S, Kim Y G, Katila N. Neuroprotective Effects of Antidepressants via Upregulation of Neurotrophic Factors in the MPTP Model of Parkinson's Disease. *Mol Neurobiol*.2018; 55(1): 554-566.
- 11.Antunes M S, Cattelan Souza L, Ladd F V L. Hesperidin Ameliorates Anxiety-Depressive-Like Behavior in 6-OHDA Model of Parkinson's Disease by Regulating Striatal Cytokine and Neurotrophic Factors Levels and Dopaminergic Innervation Loss in the Striatum of Mice. *Mol Neurobiol*.2020;57(7): 3027-3041.
- 12.Park HA, Hayden MM, Bannerman S, Jansen J, Crowe-White KM. Anti-Apoptotic Effects of Carotenoids in Neurodegeneration. *Molecules*.2020;25(15):3453.
- 13.Pan, H., Wang, Y., Na, K., Wang, Y., Wang, L., Li, Z., Guo, C., Guo, D., and Wang, X. Autophagic flux disruption contributes to Ganoderma lucidum polysaccharide-induced apoptosis in human colorectal cancer cells via MAPK/ERK activation. *Cell Death Dis*.2019;10: 456.

14. Yong, Y.X., Yang, H., Lian, J., Xu, X.W., Han, K., Hu, M.Y., Wang, H.C., and Zhou, L.M. Up-regulated microRNA-199b-3p represses the apoptosis of cerebral microvascular endothelial cells in ischemic stroke through down-regulation of MAPK/ERK/EGR1 axis. *Cell Cycle*.2019;18:1868-1881.
15. Zuo, H., Lin, T., Wang, D., Peng, R., Wang, S., Gao, Y., Xu, X., Zhao, L., Wang, S., and Su, Z. RKIP Regulates Neural Cell Apoptosis Induced by Exposure to Microwave Radiation Partly Through the MEK/ERK/CREB Pathway. *Mol Neurobiol*.2015;51:1520-1529.
16. Mu, J., Wang, R., Li, G., Li, B., and Wang, Z. Midazolam accelerates memory deterioration and neuron apoptosis of Alzheimer's disease model rats via PKA-ERK-CREB signaling pathway. *Panminerva Med*.2020.
17. Liang JQ., He JC. Effect of compound Dihuang Granule on neurobehavior of parkinsonian dyskinesia model rats with Yin deficiency and moving wind syndrome. *Chinese PLA medical Journal*.2018;43(8):652-656.
18. Wang L, Yang YF, Chen L, He ZQ, Bi DY, Zhang L, Xu YW, He JC. Compound Dihuang Granule Inhibits Nigrostriatal Pathway Apoptosis in Parkinson's Disease by Suppressing the JNK/AP-1 Pathway. *Front Pharmacol*.2021;12:621359.
19. Liang JQ, Wang L, He JC, Hua XD. Verbascoide promotes the regeneration of tyrosine hydroxylase-immunoreactive neurons in the substantia nigra. *Neural Regen Res*. 2016;11(1):101-6.
20. Prasad, E.M., & Hung, S.Y. Behavioral Tests in Neurotoxin-Induced Animal Models of Parkinson's Disease. *Antioxidants (Basel)*.2020;9(10):1007.
21. Gao, B. Y., Sun, C. C., Xia, G. H., Zhou, S. T., Zhang, Y., Mao, Y. R., Liu, P. L., Zheng, Y., Zhao, D., Li, X. T., Xu, J., Xu, D. S., & Bai, Y. L. Paired associated magnetic stimulation promotes neural repair in the rat middle cerebral artery occlusion model of stroke. *Neural Regen Res*. 2011;15(11):2047-2056.
22. Hausser, N., Johnson, K., Parsley, M. A., Guptarak, J., Spratt, H., & Sell, S. L. Detecting Behavioral Deficits in Rats After Traumatic Brain Injury. *J Vis Exp*.2018; 131: 56044.
23. Suo, N., Guo, Y. E., He, B., Gu, H., & Xie, X. Inhibition of MAPK/ERK pathway promotes oligodendrocytes generation and recovery of demyelinating diseases. *Glia*.2019; 67(7):1320-1332.
24. Zuo, H., Lin, T., Wang, D., Peng, R., Wang, S., Gao, Y., Xu, X., Zhao, L., Wang, S., and Su, Z. RKIP Regulates Neural Cell Apoptosis Induced by Exposure to Microwave Radiation Partly Through the MEK/ERK/CREB Pathway. *Mol Neurobiol*.2015;51:1520-1529.
25. Tong, H., Zhang, X., Meng, X., Lu, L., Mai, D., and Qu, S. Simvastatin Inhibits Activation of NADPH Oxidase/p38 MAPK Pathway and Enhances Expression of Antioxidant Protein in Parkinson Disease Models. *Front Mol Neurosci*.2018;11:165.

- 26.Chang, Y. M., Manoj, K. M., Lu, C. Y., Te, T. C., Tsai, C. C., Liao, P. H., Lin, S. L., Chang, C. C., Mahalakshmi, B., Kuo, W. W., & Huang, C. Y. Parkinson's disease a futile entangle of Mankind's credence on an herbal remedy: A review. *Life Sci* .2020;257:118019.
- 27.Xu PH, He, JC, Wang L, Cui XY. Clinical efficacy observation of compound Dihuang Decoction combined with Madopa in the treatment of Parkinson's disease. *Chinese Journal of Traditional Chinese Medicine*.2019;34 (2): 838-840.
- 28.Tayarani-Najaran, Z., Hadipour, E., Seyed, M. S., Emami, S. A., Mohtashami, L., & Javadi, B. Protective effects of *Lavandula stoechas* L. methanol extract against 6-OHDA-induced apoptosis in PC12 cells. *J Ethnopharmacol* .2021;273:114023.
- 29.Jiang, Y. N., Guo, Y. Z., Lu, D. H., Pan, M. H., Liu, H. Z., Jiao, G. L., Bi, W., Kurihara, H., Li, Y. F., Duan, W. J., He, R. R., & Yao, X. S. Tianma Gouteng granules decreases the susceptibility of Parkinson's disease by inhibiting ALOX15-mediated lipid peroxidation. *J Ethnopharmacol*.2020;256:112824.
- 30.Cao, C., Xiao, J., Liu, M., Ge, Z., Huang, R., Qi, M., Zhu, H., Zhu, Y., & Duan, J. A. Active components, derived from Kai-xin-san, a herbal formula, increase the expressions of neurotrophic factor NGF and BDNF on mouse astrocyte primary cultures via cAMP-dependent signaling pathway. *J Ethnopharmacol*.2018;224: 554-562.
- 31.Mohamed, E. A., Ahmed, H. I., Zaky, H. S., & Badr, A. M. Sesame oil mitigates memory impairment, oxidative stress, and neurodegeneration in a rat model of Alzheimer's disease. A pivotal role of NF-kappa B/p38MAPK/BDNF/PPAR-gamma pathways. *J Ethnopharmacol*.2021;267:113468.
- 32.Banjara, S., Suraweera, C. D., Hinds, M. G., & Kvensakul, M. The Bcl-2 Family: Ancient Origins, Conserved Structures, and Divergent Mechanisms. *Biomolecules*.2020; 10(1) :128.
- 33.Finlay, D., Teriete, P., Vamos, M., Cosford, N., & Vuori, K. Inducing death in tumor cells: roles of the inhibitor of apoptosis proteins. *F1000Res*.2017; 6:587.

## Tables

Due to technical limitations, table 1 and 2 is only available as a download in the Supplemental Files section.

## Figures

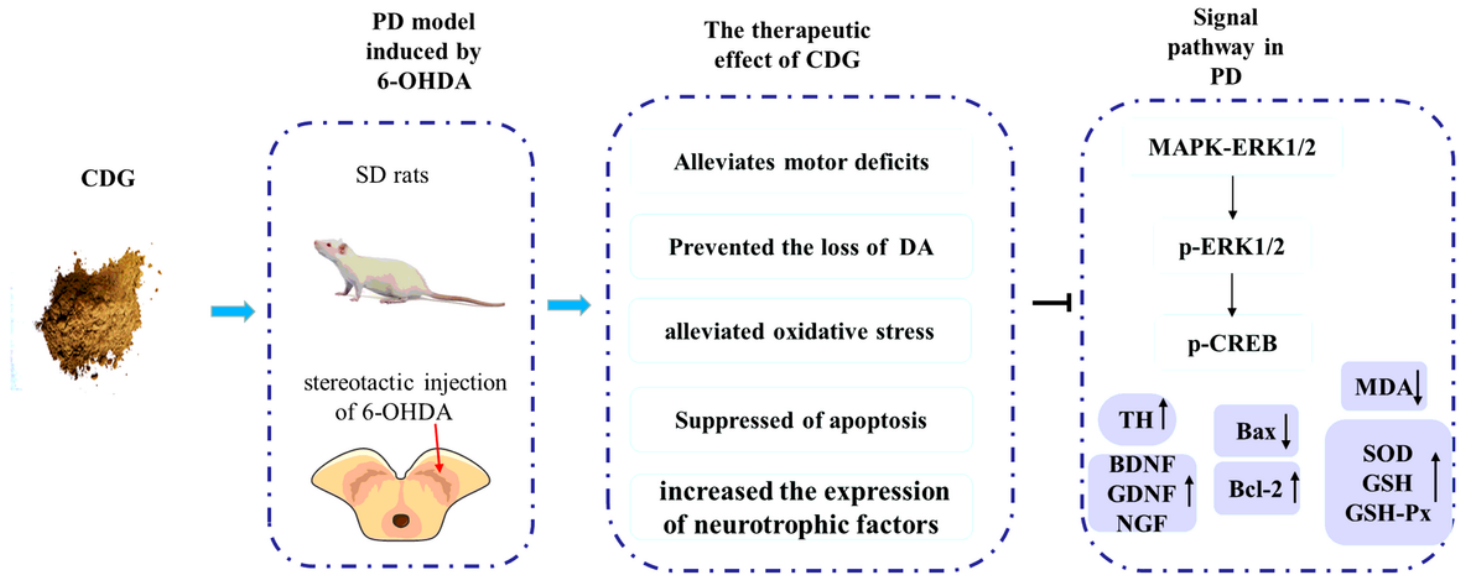
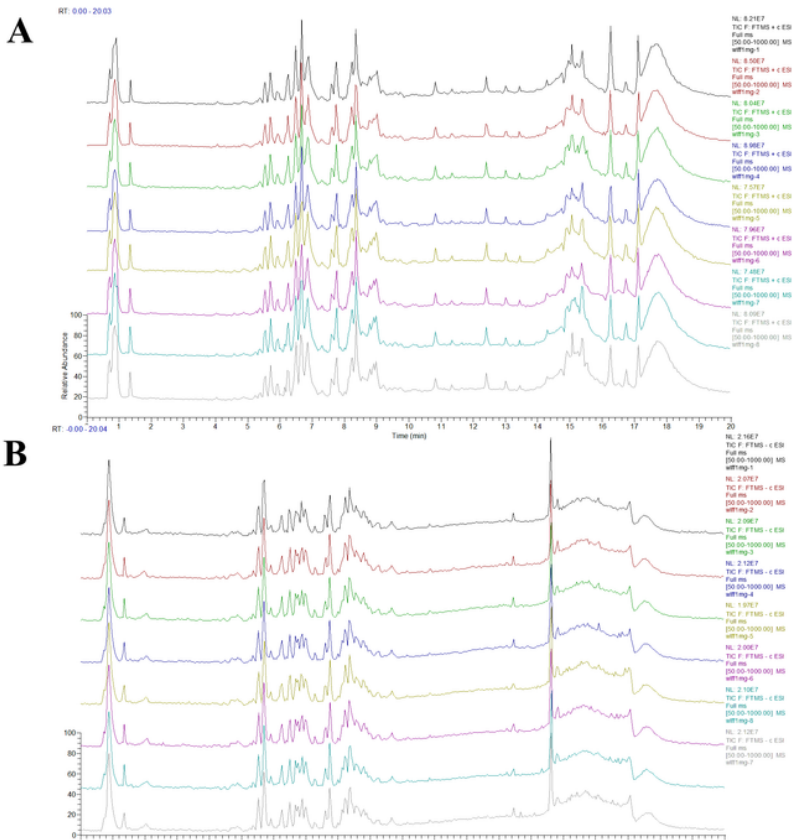


Figure 1

Experimental design of the study.



## Figure 2

The Liquid chromatography- mass spectrometry (LC-MS) analysis of CDG and the comparison of 10 different times of CDG. (A) The normal mode of CDG. (B)The negative ion mode of CDG.

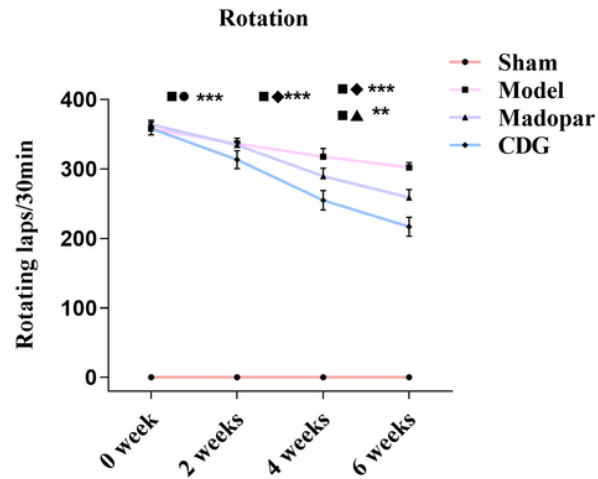


## Figure 3

CDG ameliorated behavioral symptoms of 6-OHDA induced PD rats at 0 week, 2 weeks, 4 weeks and 6 weeks. statistical analysis was performed with repeated measures and multivariate analysis of variance (ANOVA), n = 9. Significant differences were indicated by \*  $P \leq 0.05$ ; \*\*  $P \leq 0.01$ ; \*\*\*  $P \leq 0.001$ .

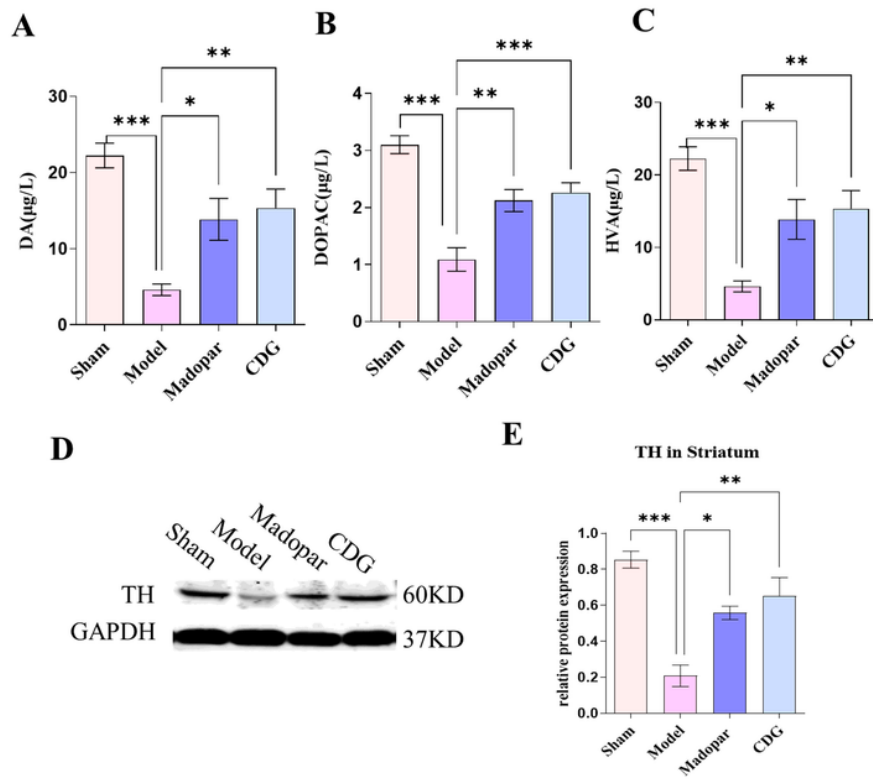


**Figure 4**

CDG attenuated nigrostriatal dopamine loss of PD rats. (A-C) DA, DOPAC and HVA were determined with HPLC-ECD. (D) The expression level of TH proteins was detected with Western Blot in the STR. (E) The expression level of TH proteins in each group. GAPDH served as control. Statistical analysis was performed with One-Way ANOVA or Two-Way ANOVA,  $n=3$ . Significant differences were indicated by \*  $P \leq 0.05$ ; \*\*  $P \leq 0.01$ ; \*\*\*  $P \leq 0.001$ .

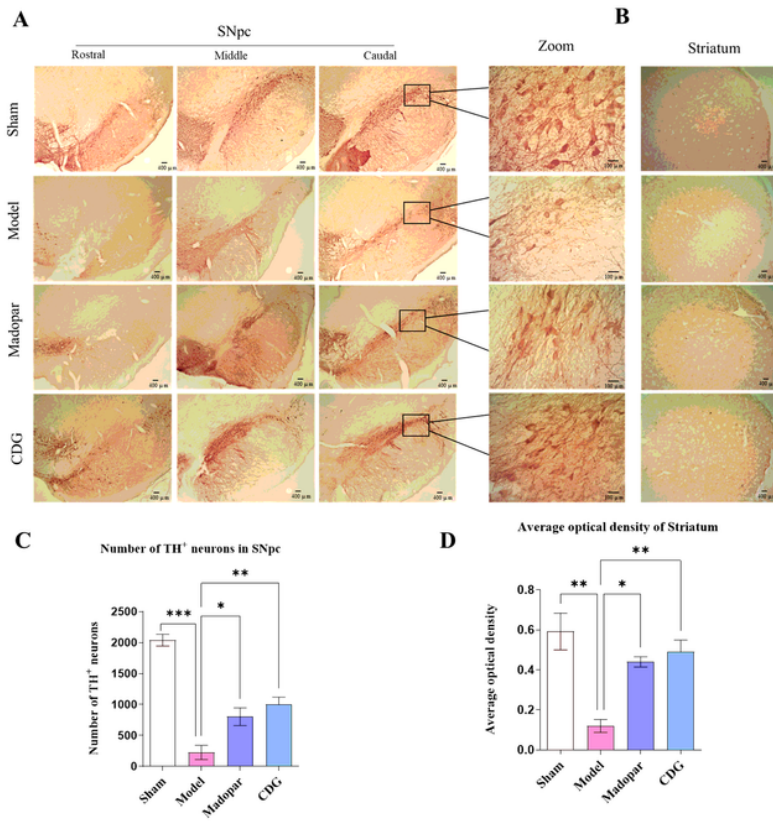


**Figure 5**

CDG attenuated 6-OHDA induced loss of nigrostriatal DA neurons in the PD rats. (A) DAB staining of TH on nigrostriatal of each group (Scale bar: 400 μm; Zoomed scale bar: 100 μm). (B) The TH-positive cells of the SNpc at 6 weeks. (C) Average optical density of the striatum of each group. Statistical analysis was performed with One-Way ANOVA or Two-Way ANOVA, n = 3. Significant differences were indicated by \* P < 0.05; \*\* P < 0.01; \*\*\* P < 0.001.

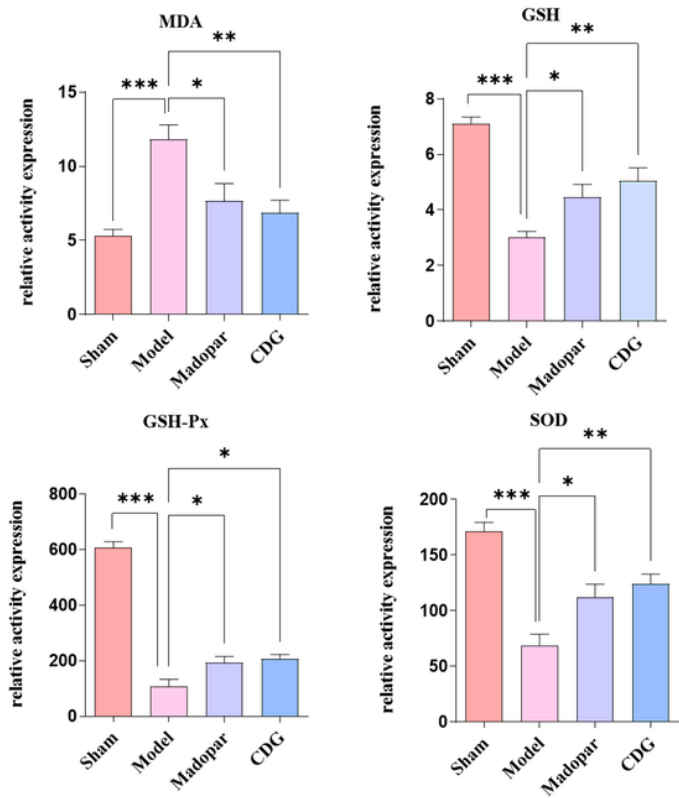


**Figure 6**

CDG alleviated 6-OHDA induced oxidative stress in the Striatum of PD rats. (A) The MDA content in the Striatum of each group. (B-C) The GSH and GSH-Px activity in each group at 6 weeks. (D) The SOD activity in each group at 6 weeks. Statistical analysis was performed with One-Way ANOVA,  $n = 3$ . Significant differences were indicated by \*  $P \leq 0.05$ ; \*\*  $P \leq 0.01$ ; \*\*\*  $P \leq 0.001$ .

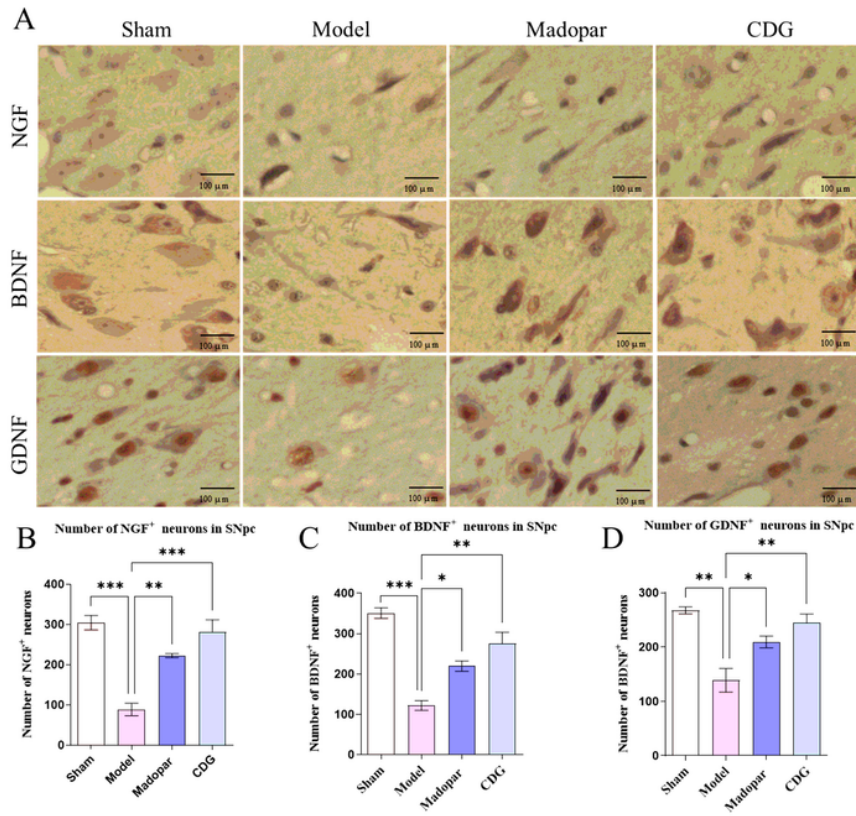


**Figure 7**

CDG increased the expression of neurotrophic factors in the SNpc of PD rats. (A) IHC staining of NGF, BDNF and GDNF on nigrostriatal of each group (Scale bar: 100  $\mu$ m). (B-D) Counts of NGF, BDNF and GDNF-positive cells of the SNpc at 6 weeks. Statistical analysis was performed with One-Way ANOVA or Two-Way ANOVA,  $n = 3$ . Significant differences were indicated by \*  $P \leq 0.05$ ; \*\*  $P \leq 0.01$ ; \*\*\*  $P \leq 0.001$ .

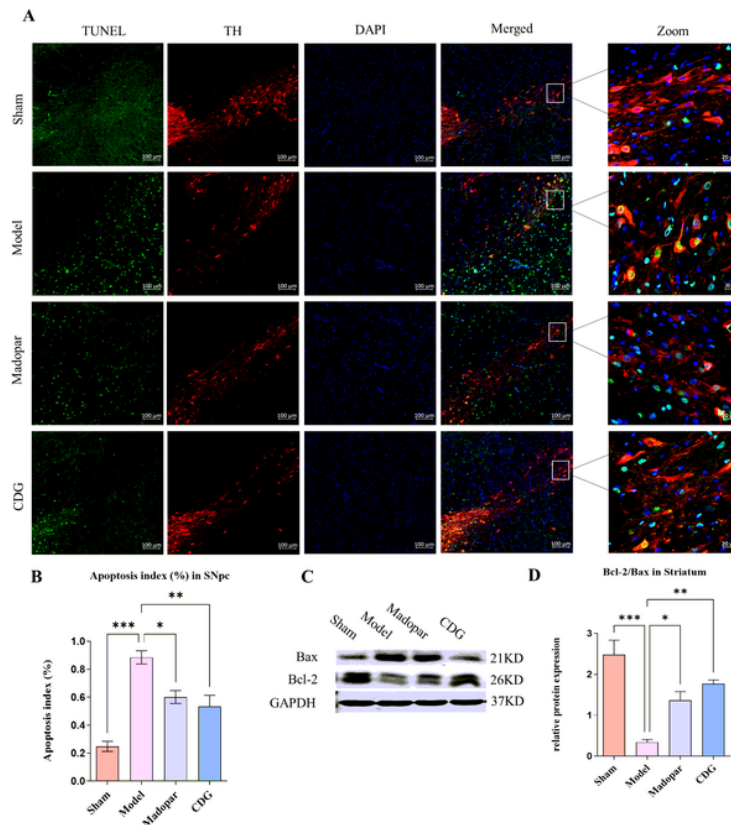


**Figure 8**

CDG reduced 6-OHDA induced cell apoptosis in the nigrostriatal pathway of PD rats. (A) TUNEL assay of the apoptotic neurons in the SNpc of rats. TUNEL (green), TH (red) and DAPI (blue). (Scale bar: 100  $\mu$ m; Zoomed scale bar: 20  $\mu$ m). (B) Apoptosis index of the SNpc in each group. (C-D) The expression level of the Bcl-2/Bax protein was detected with Western Blot in the Striatum. GAPDH served as control. Statistical analysis was performed with One-Way ANOVA, Turkey's multiple comparison test post hoc,  $n = 3$ . Statistical analysis was performed with Two-Way ANOVA,  $n = 3$ . Significant differences were indicated by \*  $P \leq 0.05$ , \*\*  $P \leq 0.01$ , \*\*\*  $P \leq 0.001$ .

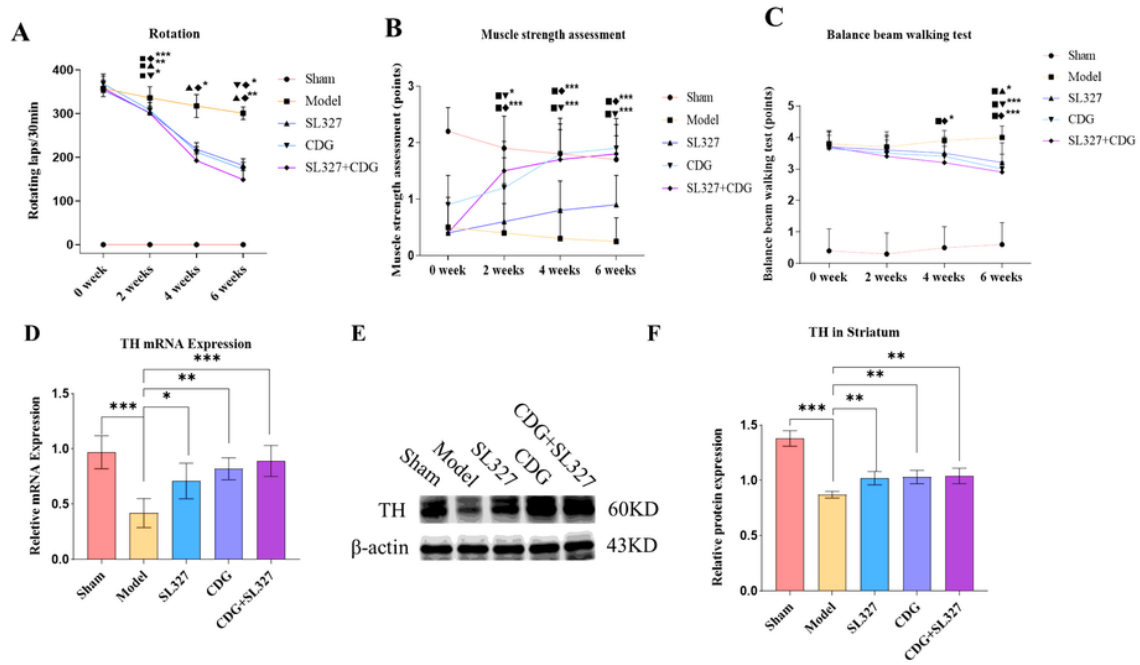


**Figure 9**

CDG and SL327 improved the Parkinsonian symptoms of 6-OHDA induced PD rats. (A) The rotation behaviors of rats with 2 weeks, 4 weeks and 6 weeks treatments. (B) The myodynamia score of rats in each group. (C) The beam test of rats in each group. (D) The mRNA expression levels of TH in each group. (E-F) The protein expression levels of TH in the Striatum.  $\beta$ -actin served as control. Statistical analyses were performed with One-Way ANOVA, Turkey's multiple comparison test post hoc. Significant differences were indicated by \*  $P < 0.05$ , \*\*  $P < 0.01$ , \*\*\*  $P < 0.001$ .

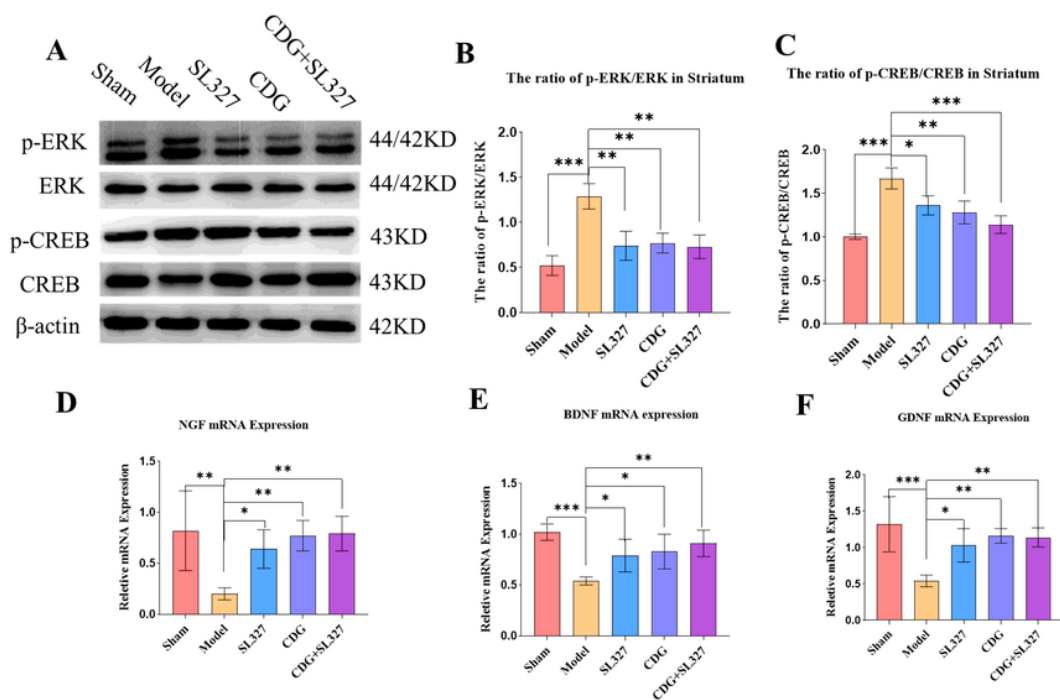


**Figure 10**

CDG inhibited the phosphorylation of MAPK/ERK1/2 induced by 6-OHDA. (A) Protein Expression levels of ERK, p-ERK, CREB, p-CREB proteins in the Striatum of rats.  $\beta$ -actin served as control. (B-F) The statistical analyses of protein expression levels of each group. (D-F) The mRNA levels of NGF, BDNF and GDNF in each group.  $\beta$ -actin served as control. Statistical analyses were performed with One-Way ANOVA, Turkey's multiple comparison test post hoc. Significant differences were indicated by \*  $P \leq 0.05$ , \*\*  $P \leq 0.01$ , \*\*\*  $P \leq 0.001$ .

## Supplementary Files

This is a list of supplementary files associated with this preprint. Click to download.

- [Table1.tif](#)
- [Table2.tif](#)